
Proc. XXXVII International School of Semiconducting Compounds, Jaszowiec 2008

Study of the Defect Structure of $\text{Hg}_{1-x}\text{Cd}_x\text{Te}$ Films by Ion Milling

M. POCIASK^a, I.I. IZHININ^b, E.S. ILYINA^b, S.A. DVORETSKY^c,
N.N. MIKHAILOV^c, YU.G. SIDOROV^c, V.S. VARAVIN^c
AND K.D. MYNBAEV^d

^aInstitute of Physics, University of Rzeszów
Rejtana 16A, 35-310 Rzeszów, Poland

^bR&D Institute for Materials SRC "Carat", Lviv, 79031, Ukraine

^cA.V. Rzhanov Institute of Semiconductor Physics of SB RAS
Novosibirsk, 623900, Russia

^dA.F. Ioffe Physico-Technical Institute of RAS
St.-Petersburg, 194021, Russia

A study of the defect structure of heteroepitaxially grown $\text{Hg}_{1-x}\text{Cd}_x\text{Te}$ (MCT) films was performed with the use of ion milling. Undoped and *in situ* As- (acceptor) or In- (donor) doped films with $x = 0.22$, grown by molecular beam epitaxy on GaAs substrates, as-grown and annealed, were subjected to ion milling with subsequent electrical characterization. The results obtained on the MBE films were compared to those acquired on wafers cut from bulk crystals, and on epitaxial films grown by liquid and vapor phase epitaxy. In all the MBE films ion milling revealed a presence of a neutral defect with concentration $\approx 10^{17} \text{ cm}^{-3}$, formed at the stage of the growth. Residual donor concentration in the films was found to be of the order of 10^{15} cm^{-3} , which is typical of high-quality MCT.

PACS numbers: 73.61.Ga, 61.80.Jh, 66.30.Lw

1. Introduction

$\text{Hg}_{1-x}\text{Cd}_x\text{Te}$ (MCT) semiconductors still hold their position as the standard material for infrared detection, especially in the long-wave region of the spectrum. Of the many techniques used to characterize the quality of MCT, ion milling is emerging as unique means to reveal electrically active defects and complexes. It is known that ion milling is capable of strongly affecting electrical properties of MCT, and may cause conductivity type conversion in p-type material or decrease in the degree of electrical compensation in n-type MCT [1]. This effect is now

widely used in MCT technology, when ion milling is employed for fabrication of p - n junctions in vacancy- and acceptor-doped-type material. It appeared also that strongly non-equilibrium processes which take place under ion milling, when a crystal is oversaturated with interstitial mercury atoms Hg_I [2, 3], allowed one to detect defects that did not show their presence before the milling because of electrical compensation [4, 5]. The character of post-milling relaxation of electrical properties of MCT allows for identifying background dopants, which are hard to detect using secondary-ion mass-spectroscopy (SIMS) [6].

MCT structures grown by molecular beam epitaxy (MBE) have become a basic material for developing infrared focal plane arrays, including those for third-generation infrared detectors [7–9]. Though MBE MCT technology is now quite mature, it still faces a number of challenges related to the presence of a considerable number of structural and point defects in the films grown on foreign (GaAs or Si) substrates. These defects may have detrimental effect on the properties of device structures and revealing them is a topical task.

In this paper, we report on the results of a study of the defect structure of heteroepitaxial MBE MCT films with the use of ion milling. We have studied nominally undoped structures and those *in situ* doped with acceptor (As with concentration 10^{15} – 10^{16} cm^{-3}) or donor (In with concentration 5×10^{14} – 10^{17} cm^{-3}) dopants, both as-grown and after post-growth annealing. We compared the results obtained on the MBE films to those acquired on MCT bulk crystals and epitaxial films grown by liquid and vapor phase epitaxy. Using ion milling allowed us to detect in all the MBE films studied a neutral defect with concentration $\approx 10^{17}$ cm^{-3} , and to make estimates of background dopant concentration.

2. Experiment

The heteroepitaxial MBE structures were grown on (013) CdTe/ZnTe/GaAs substrates [8]. In a typical MBE structure, a $\text{Hg}_{1-x}\text{Cd}_x\text{Te}$ ($x = 0.22$) “absorber” film with a thickness $d \approx 8$ – 10 μm was protected by ≈ 0.3 μm thick (top) and ≈ 1.0 μm thick (bottom) graded-gap films with x increasing up to ≈ 0.4 near the both interfaces.

The electrical properties of the samples were studied by measuring the Hall coefficient R_H and conductivity σ in magnetic field B of 0.01 up to 1.5 T at the temperature $T = 77$ K. The measurements were performed on square-shaped van der Pauw structures. The $R_\text{H}(B)$ and $\sigma(B)$ dependences were analyzed using discrete mobility spectrum analysis (DMSA) [10].

The undoped as-grown structures used for fabricating p -type films (samples ##1, 2) were of n -type conductivity with electron concentration and mobility $n_{77} \approx 2 \times 10^{14}$ cm^{-3} and $\mu_{n77} \approx 10^5$ $\text{cm}^2/(\text{V s})$ at 77 K, respectively. They were converted into p -type (vacancy-doped) by an annealing in He atmosphere at 210°C for 24 h. The hole concentration p_{77} and mobility μ_{p77} after the annealing are given in Table I, where d is the thickness of the MCT film/wafer.

TABLE I

Parameters of *p*-type samples studied in this work.

Sample	#1	#2	#3	#4	#5	#6	#7	#8
Growth method	MBE, undoped	MBE, undoped	MBE, As-doped	MBE, As-doped	LPE, undoped	VDC, undoped	VDC, Se-doped	VDC, Cu-doped
x	0.22	0.22	0.22	0.22	0.22	0.28	0.22	0.22
d [μm]	10.1	10.75	8.0	8.2	18.8	815	990	1020
after annealing, before ion milling								
$p_{77} \times 10^{-16}$ [cm^{-3}]	1.0	0.8	1.0	1.2	1.6	1.3	0.3	1.9
μ_{p77} [$\text{cm}^2/(\text{V s})$]	500	480	400	420	510	380	420	470
Directly after ion milling								
$n_{77} \times 10^{-16}$ [cm^{-3}]	14	11	16	18	2.3	2.6	0.1	1.0
μ_{n77} [$\text{cm}^2/(\text{V s})$]	48000	53000	41900	41000	92000	25000	110000	69000

The As-doped as-grown films (samples ##3, 4) were also of *n*-type conductivity with $n_{77} \approx (8-9) \times 10^{15} \text{ cm}^{-3}$ and $\mu_{n77} \approx 5 \times 10^4 \text{ cm}^2/(\text{V s})$. A two-stage thermal annealing (360°C (2 h) and 210°C (24 h) under Hg saturation) was used to activate the As acceptor. As a result of the annealing, the films were converted into *p*-type with $p_{77} \approx 10^{16} \text{ cm}^{-3}$ and $\mu_{p77} \approx 400 \text{ cm}^2/(\text{V s})$ (see Table I). This meant a 100%-efficient dopant activation, since the As concentration in the films, as determined by SIMS, was of the order of 10^{16} cm^{-3} . Ion milling was also applied to a liquid phase epitaxy (LPE) film grown from Te-rich solution on a CdZnTe substrate (sample #5), and to MCT wafers cut from bulk ingots grown by vertical-directed crystallization (VDC) with replenishment from the solid phase (samples ##6-8). Sample #7 was doped with Se ($\approx 1 \text{ at.}\%$) during the growth. Sample #8 was post-growth doped with Cu using the doping scheme described elsewhere [10]. After the growth, the LPE and bulk samples were annealed in saturated Hg vapors, the resulting p_{77} and μ_{p77} values are given in Table I.

n-type structures were either undoped MBE films that did not undergo post-growth annealing, or films *in situ* doped with In. The In concentration in the samples was 5×10^{14} to 10^{17} cm^{-3} . The parameters of the structures are given in Table II.

Ion milling was performed using an IB-3 (EIKO, Japan) etching system with Ar^+ ion energy 500 eV, current density 0.1–0.2 mA/cm², and milling time 20 min. The sample temperature during the milling was kept at $\approx 293 \text{ K}$ by means of cooling of the sample holder with water. Relaxation of electrical properties of the samples after the milling was studied through aging them in air at $293 \pm 2 \text{ K}$.

3. Results

Ion milling of the annealed MBE and LPE *p*-type films resulted in *p*-to-*n* conductivity type conversion throughout their whole thickness. In bulk samples an

TABLE II

Parameters of n -type samples studied in this work.

Sample	#10	#11	#12	#13	#14
Doping	–	In	In	In	In
As-grown (before ion milling)					
n_{77} [cm^{-3}]	7.6×10^{13}	3.2×10^{14}	2.2×10^{15}	1.3×10^{16}	1.1×10^{17}
μ_{n77} [$\text{cm}^2/(\text{V s})$]	163000	166000	110000	71000	32600
Directly after ion milling					
$n_{77} \times 10^{-17}$ [cm^{-3}]	1.1	0.96	1.0	1.3	2.4
μ_{n77} [$\text{cm}^2/(\text{V s})$]	55300	61600	50700	45400	28600
After relaxation					
t [min]	186810	58060	185770	185870	105000
n_{77} [cm^{-3}]	2.4×10^{15}	2.3×10^{15}	4.7×10^{15}	1.6×10^{16}	1.1×10^{17}
μ_{n77} [$\text{cm}^2/(\text{V s})$]	137000	111350	101000	70600	32800

n -type converted layer was formed; its thickness was determined using step-by-step chemical etching. In all the samples, the converted layer represented typical n^+-n structure [1], which comprised a radiation-damaged n^+ -“surface” layer ($\approx 2 \mu\text{m}$ in thickness) and a “bulk” n -layer.

During the aging, we observed substantial changes of the R_H and σ for all the samples. Figure 1 shows an example of evolution of a mobility spectrum envelope [10] for the vacancy-doped MBE film #2 during the aging. It is seen that before the milling (curve 1) the conductivity of the sample was determined by both heavy and light holes. After the milling, the spectrum became dominated by the peaks corresponding to high-mobility electrons, which could be related to the formation of the “bulk” n -layer (curve 2). With aging (curves 3 to 5), the mobility of these electrons was increasing, but their contribution to the conductivity was decreasing. As a result, the contribution to σ of low-mobility electrons, which could be associated with the damaged “surface” n^+ -layer, became noticeable. At a certain transition aging stage (curve 5), the contribution of the low-mobility electrons to the conductivity became comparable to that of the high-mobility electrons. After a $0.7 \mu\text{m}$ thick radiation-damaged layer was chemically removed from the surface, the mobility spectrum again became dominated by the peak corresponding to the high-mobility electrons (curve 6). This meant also that the high-mobility electrons were indeed those of the “bulk” converted n -layer.

The n_{77} and μ_{n77} values in the “bulk” converted layers of the samples as measured directly after the milling are given in Table I. It is seen that the n_{77}

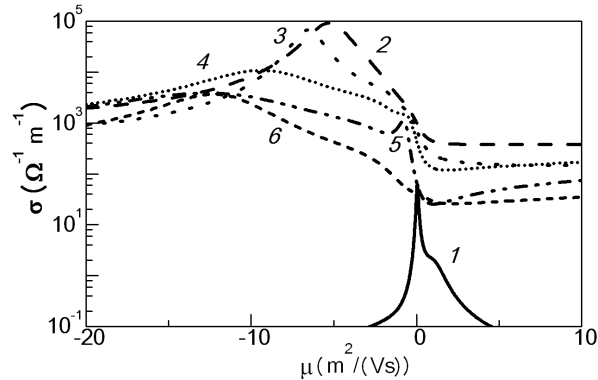


Fig. 1. Envelopes of mobility spectra at 77 K for the MBE film #2: annealed sample (1), after ion milling and ageing for 20 (2), 200 (3), 1380 (4), 231600 (5) min, and after removing 0.7 μm thick surface layer by chemical etching (6).

in all the MBE films was of the order of 10^{17} cm^{-3} , irrespective of the type and the level of acceptor doping. In the vacancy-doped bulk and LPE samples the n_{77} was lower by almost an order of magnitude ($\approx 2 \times 10^{16} \text{ cm}^{-3}$). In the Se-doped sample it was still lower ($\approx 1.5 \times 10^{15} \text{ cm}^{-3}$).

Figure 2 summarizes the data on the relaxation of the n_{77} in the vacancy-doped samples after the milling. The dependence of the n_{77} on the aging time for all the samples was tri-exponential, which is typical of disintegration of donor centers (complexes) formed under ion milling [6]. The fitting curves are shown in Fig. 2 by solid lines. In the Se-doped sample after ≈ 1000 min of aging the contribution of electrons into the conductivity of the “bulk” converted layer became negligibly small.

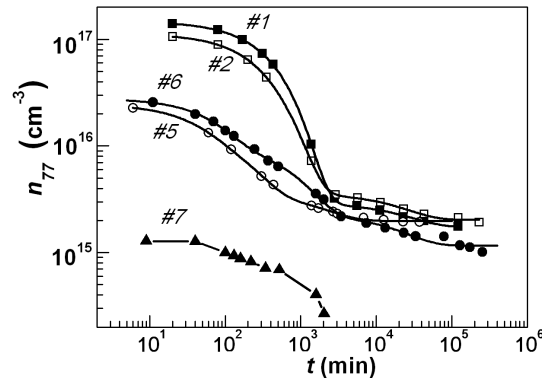


Fig. 2. Aging time dependence of the electron concentration in the “bulk” converted n -layer for the vacancy-doped MBE films (##1, 2), and LPE (#5) and bulk (##6, 7) MCT samples.

Relaxation of the n_{77} in the ion-milled As-doped MBE films and the Cu-doped bulk sample is shown in Fig. 3. For comparison, we also present here the data on the relaxation of n_{77} in ion-milled As-doped MCT sample (#9) grown by isothermal vapor-phase epitaxy (ISOVPE) [11]. For all the samples involved in the current study the decrease in the n_{77} upon the aging at 300 K did not lead to re-conversion into p -type.

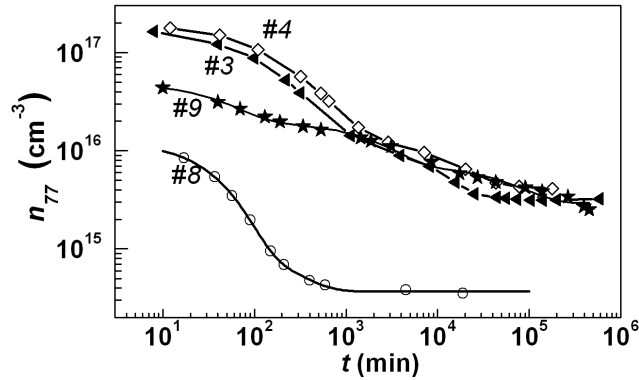


Fig. 3. Aging time dependence of the electron concentration in the “bulk” converted n -layer for the As-doped MBE films (##3, 4), Cu-doped bulk MCT sample (#8), and As-doped ISOVPE film (#9).

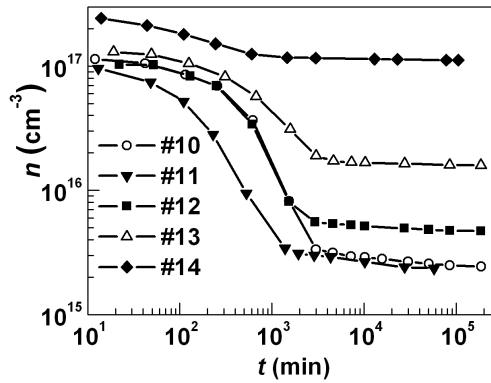


Fig. 4. Aging time dependence of the electron concentration in initially n -type structures.

Ion milling of the n -type MBE films resulted in modification of the electrical properties of the films throughout their whole thickness. Similar to the p -type films, in all the samples the modified layer represented an $n^+ - n$ structure, which comprised a radiation-damaged n^+ -“surface” layer and a “bulk” n -layer. The n_{77} and μ_{n77} in the “bulk” n -layers of the films as measured directly after ion milling

are given in Table II. Again, the n_{77} in all the films was of the order of 10^{17} cm^{-3} , irrespective of concentration of donors introduced during the growth.

Figure 4 shows relaxation of the n_{77} in the structures after the milling. The dependence of the n_{77} on the aging time t for all these samples was bi-exponential.

4. Discussion

According to the existing concept [6, 11, 12], in extrinsically acceptor-doped MCT the Hg_I atoms released by ion milling form donor centers, whose concentration $[D\cdot]$ is expressed by the equation

$$[D\cdot] = \frac{[\text{Hg}_I]}{[\text{Hg}_I] + K_X} [A_X], \quad (1)$$

where $[\text{Hg}_I]$ is Hg_I concentration; $[A_X]$ is acceptor dopant concentration, and K_X is the equilibrium constant for a reaction of the center formation. Since during a typical milling process $[\text{Hg}_I] \approx 10^{13}\text{--}10^{14} \text{ cm}^{-3}$ and $K_X \approx 10^9 \text{ cm}^{-3}$ [2, 3], $[\text{Hg}_I] \gg K_X$ and $[D\cdot]$ directly after ion milling should be equal to $[A_X]$. It was this trend that we observed in ion-milled As-doped ISOVPE layers and Cu(Ag, Au)-doped bulk MCT [6, 11, 12]. For example, the p_{77} , which reflected dopant concentration in the Cu- and As-doped samples was $2 \times 10^{16} \text{ cm}^{-3}$ and $4 \times 10^{16} \text{ cm}^{-3}$, respectively, and so was the n_{77} in these samples directly after the milling (Fig. 3, curves 8 and 9). After ion milling $[\text{Hg}_I] \ll K_X$ and the centers disintegrate.

Following this concept, in vacancy-doped samples straight after ion milling the n_{77} should be equal to the total concentration of all electrically active residual dopants (both donors and acceptors). In reality, the n_{77} values in Table I for the undoped LPE and bulk MCT samples ## 5,6 appeared to be 2 to 3 times higher than the estimations of residual dopant concentration in the samples [13, 14]. Low electron concentration in the Se-doped sample #7 is explained by the fact that the presence of Se reduces residual impurity concentration in MCT [15].

In the As-, In- and vacancy-doped MBE films the electron concentration after the milling appeared to be of the order of 10^{17} cm^{-3} . For the As- and vacancy-doped structures, this value was 1 and 2 orders higher than the As doping level or estimated residual dopant concentration, respectively. Therefore, the high n_{77} after the milling cannot be explained solely by the interaction of Hg_I with the electrically active acceptor dopants, be them residual or intentionally (As) introduced. Thus, we can develop our earlier suggestion [16] that in our MBE films ion milling leads to the formation of donor centers, which result from the interaction of Hg_I with certain defects that were electrically neutral before the milling. Since these defects were activated in all the MBE structures, irrespective of type and level of doping, they should have formed during the growth, and still kept neutral after the annealing. The latter fact may mean that they represent complex native defects [17], or initially electrically neutral impurity. Such an impurity might be, for example, oxygen, which can act in MCT as a donor [18]. The SIMS study performed on the MBE films did reveal the presence of oxygen

with concentration about 10^{17} cm^{-3} , so it is quite possible that the defect activated by the ion milling is a residual impurity such as oxygen. According to the results presented in Table I and Fig. 2, we can also imply the presence of similar defects, though in smaller quantities, in the bulk and LPE samples.

As to the electron concentration in the samples after the relaxation, it is easy to see that in all the samples with initial p -type (except for samples ##7 and 8), regardless of the doping method and the doping level, the n_{77} stabilized at the level of $(1-3) \times 10^{15} \text{ cm}^{-3}$. This value should reflect the background donor level in the samples, since after the relaxation most of the acceptor centers transform into neutral form [19]. Thus, one can see that the residual donor concentration in our MBE films is of the order of 10^{15} cm^{-3} , which (see samples ##5, 6 and 9) is typical of high-quality MCT.

Regarding the relaxation in n -type samples, it follows from Fig. 4 that after $\approx 10^4$ min of aging the n_{77} in the In-doped structures with indium concentration $N_{\text{In}} \geq 10^{16} \text{ cm}^{-3}$ stabilized at the level of the introduced dopant. This means that indium doping can be effectively used for defining the level of electron concentration in n -regions of MCT-based device structures fabricated with the use of ion milling. In nominally undoped sample #10 and In-doped sample #11 with $N_{\text{In}} = 4.2 \times 10^{14} \text{ cm}^{-3}$, the n_{77} stabilized at $\approx (2-4) \times 10^{15} \text{ cm}^{-3}$. This confirms that the residual donor concentration in our MBE films is indeed of the order of 10^{15} cm^{-3} .

5. Conclusions

In conclusion, we applied ion milling for the study of defects in heteroepitaxial MCT films grown on GaAs by molecular beam epitaxy. By measuring electrical properties of the films before and after the milling, we revealed the presence of specific neutral defects with high concentration (10^{17} cm^{-3}). It can be speculated that these defects form during the growth and are impurity-related. The concentration of residual donors in the films, according to the data obtained with the use of ion milling, was of the order of 10^{15} cm^{-3} , which is typical of high-quality MCT material. These results show that ion milling can be used as an effective tool for defect structure diagnostics in MCT.

Acknowledgments

This work was partly supported by Ministry of Education and Science of Ukraine under contract No. M/184-2007, by RFBR grant No. 07-02-00400, and by Integration project of SB RAS No. 3.20.

References

- [1] K.D. Mynbaev, V.I. Ivanov-Omskii, *Semiconductors* **37**, 1127 (2003).
- [2] V.V. Bogoboyashchii, I.I. Izhnin, *Russian Phys. J.* **43**, 627 (2000).

- [3] D. Shaw, P. Capper, *J. Mater. Sci.: Mater. Electron.* **11**, 169 (2000).
- [4] V.I. Ivanov-Omskii, K.E. Mironov, K.D. Mynbaev, *Semicond. Sci. Technol.* **8**, 634 (1993).
- [5] V.V. Bogoboyashchyy, S.A. Dvoretzky, I.I. Izhnin, N.N. Mikhailov, Yu.G. Sidorov, F.F. Sizov, V.S. Varavin, V.A. Yudenkov, *Phys. Status. Solidi C* **1**, 355 (2004).
- [6] I.I. Izhnin, V.V. Bogoboyashchyy, F.F. Sizov, *Proc. SPIE* **5881**, 222 (2005).
- [7] R. Haakenaasen, H. Steen, E. Selvig, T. Lorentzen, A.D. Van Rheenen, L. Trosdahl-Iversen, H. Syversen, D. Hall, N. Gordon, T. Skauli, A.H. Vaskinn, *Phys. Scr.* **126**, 31 (2006).
- [8] V.S. Varavin, V.V. Vasiliev, S.A. Dvoretzky, N.N. Mikhailov, V.N. Ovsyuk, Yu.G. Sidorov, A.O. Suslyakov, M.V. Yakushev, A.L. Aseev, *Opto-Electron. Rev.* **11**, 99 (2003).
- [9] F. Aqariden, P.D. Dreiske, M.A. Kinch, P.K. Liao, T. Murphy, H.F. Schaake, T.A. Shafer, H.D. Shin, T.H. Teherani, *J. Electron. Mater.* **36**, 900 (2007).
- [10] V.V. Bogoboyashchyy, A.I. Elizarov, I.I. Izhnin, *Semicond. Sci. Technol.* **20**, 726 (2005).
- [11] V.V. Bogoboyashchyy, I.I. Izhnin, K.D. Mynbaev, M. Pociask, A.P. Vlasov, *Semicond. Sci. Technol.* **21**, 1144 (2006).
- [12] I.I. Izhnin, V.V. Bogoboyashchyy, M. Pociask, K.D. Mynbaev, V.I. Ivanov-Omskii, *Semiconductors* **41**, 804 (2007).
- [13] V.V. Bogoboyashchyy, *Semiconductors* **36**, 1332 (2002).
- [14] V.V. Bogoboyashchyy, K.R. Kurbanov, A.P. Oksanich, *Funct. Mater.* **7**, 546 (2000).
- [15] V.V. Bogoboyashchyy, I.I. Izhnin, K.R. Kurbanov, UA Patent No. 54476 (2003).
- [16] I.I. Izhnin, S.A. Dvoretzky, N.N. Mikhailov, Yu.G. Sidorov, V.S. Varavin, K.D. Mynbaev, M. Pociask, *Appl. Phys. Lett.* **91**, 132106 (2007).
- [17] M.L. Young, J. Giess, *J. Appl. Phys.* **69**, 7173 (1991).
- [18] M. Yoshikawa, S. Ueda, K. Maruyama, H. Takigawa, *J. Vac. Sci. Technol. A* **3**, 153 (1985).
- [19] E. Belas, R. Grill, J. Franc, P. Moravec, R. Varghová, P. Höschl, H. Sitter, *J. Cryst. Growth* **224**, 52 (2001).